HOSTED BY

ELSEVIER

Contents lists available at ScienceDirect

Saudi Journal of Biological Sciences

journal homepage: www.sciencedirect.com

الجمعية السعودية لعلوم الحياة
SAUDI BIOLOGICAL SOCIETY

Original article

# *Bacillus* sp. strain MRS-1: A potential candidate for uranyl biosorption from uranyl polluted sites

Jada Hoyle-Gardner [a,c], Veera Lakshmi Devi Badisa [a,*], Shahid Sher [b], Li Runwei [d], Benjamin Mwashote [a], Victor Ibeanusi [a]

[a] Core Laboratory, School of the Environment, Florida A&M University, Tallahassee, FL, USA
[b] Williams Lab, School of the Environment, Florida A&M University, Tallahassee, FL, USA
[c] Environmental Health, Rollins School of Public Health, Emory University, Atlanta, GA, USA
[d] Department of Civil Engineering, New Mexico State University, Las Cruces, NM, USA

ARTICLE INFO

*Keywords:*
Uranium
Toxic
Metal resistant
*Bacillus* bacteria
Biomass
Biosorption

ABSTRACT

The uranyl tolerance of a metal-resistant *Bacillus* sp. strain MRS-1, was determined in this current study. This was done due to a rise in anthropogenic activities, such as the production of uranium-based nuclear energy, which contributes to environmental degradation and poses risks to ecosystems and human health. The purpose of the research was to find effective strategies for uranium removal to minimize the contamination. In this paper, the biosorption of uranyl was investigated by batch tests. Bacteria could continue to multiply up to 350 ppm uranyl concentrations, however this growth was suppressed at 400 ppm, that generally accepted as the minimum concentration for bacterial growth inhibition. The optimal conditions for uranyl biosorption were pH 7, 20 °C, and a contact duration of 30 min with living bacteria. According to the findings of an investigation that used isotherm and kinetics models (Langmuir, Freundlich and pseudo second order), *Bacillus* sp. strain MRS-1 biosorption seemed to be dependent on monolayer adsorption as well as certain functional groups that had a strong affinity for uranyl confirmed by Fourier Transform Infrared Spectroscopy (FTIR) analysis. The shifts/sharping of peaks (1081–3304 $cm^{-1}$) were prominent in treated samples compared to control one. These functional groups could be hydroxyl, amino, and carboxyl. Our findings showed that *Bacillus* sp. strain MRS-1 has an elevated uranyl biosorption ability, with 24.5 mg/g being achieved. This indicates its potential as a powerful biosorbent for dealing with uranium contamination in drinking water sources and represents a breakthrough in the cleanup of contaminated ecosystems.

## 1. Introduction

Uranium is a radioactive, toxic, and polluting heavy metal that can cause harm to the environment. It occurs in numerous chemical and physical forms in the Earth's crust. It is present in three isotopes which are 234U (0.005 %), 235U (0.72 %), and 238U (99.27 %) (Bjørklund et al., 2020). It is found in the form of complex ores such as autunite, carnotite, pitchblende, torbernite, uraninite, and uranophane in the nature. Pitchblende and uraninite ores accounts for around 50 to 80 % of total uranium (Choppin et al., 2013). Nevertheless, uranium also released into the environment due to various anthropogenic activities such as coal combustion, nuclear plants, gold mining, nuclear weapon testing, use of natural uranium-bearing rocks and uranium-containing phosphate fertilizers (Roper et al., 2013; Liesch et al., 2015; Lakaniemi et al., 2019). Uranium is the most widely encountered radionuclide in aqueous environments compared to other radioactive pollutants, and it has a half-life of millions of years (Schnug and Lottermoser, 2013). It also can be highly accumulated in river sediments due to adsorption and biotransformation (Filistovic et al., 2015; Ivanova et al., 2015; Malikova et al., 2020). It is reported that the sediment uranium pollution has caused a serious hazard to aquatic ecosystems (Sayadi et al., 2010; Zahra et al., 2014; Portela et al., 2020). The uranium level in the groundwater varies from one area to another (Coyte and Vengosh, 2020). Uranium pollution in the ground water has been reported in

Peer review under responsibility of King Saud University. Production and hosting by Elsevier.
* Corresponding author at: School of Environment, Florida A&M University, Tallahassee, USA.
*E-mail addresses:* jada.hoylegardner@famu.edu (J. Hoyle-Gardner), veera.badisa@famu.edu (V.L.D. Badisa), shahid.sher@famu.edu (S. Sher), rl25@nmsu.edu (L. Runwei), benjamin.mwashote@famu.edu (B. Mwashote), victor.ibeanusi@famu.edu (V. Ibeanusi).

https://doi.org/10.1016/j.sjbs.2023.103873
Received 9 October 2023; Received in revised form 27 October 2023; Accepted 10 November 2023
Available online 11 November 2023

various countries such as Argentina (Matteoda et al., 2019), Brazil (Godoy et al., 2019), India (Pant et al., 2019), and Pakistan (Ali et al., 2019). Uranyl ion salts, which are more soluble than uraninite, predominate in oxic conditions because of their interaction with carbonate, phosphate, and sulphate groups (Echevarria et al., 2001; Cumberland et al., 2016). It can eventually make its way into drinking water and food chain from the polluted environment. In shellfish from the USA and UK, the greatest quantities of uranium ranging between 9.5 and 31 μg/kg were observed (EFSA, 2009). The issue of uranium pollution is a considerable apprehension at numerous sites operated by the United States Department of Energy (Li et al., 2014). Uranium pollution poses a substantial risk to human health and the ecosystem because of high radiotoxicity and chemotoxicity (Gao et al., 2019; Rump et al., 2019). After exposure to uranium, it enters the blood stream, accumulates in various organs of human body and has been reported to cause the diseases in kidney, blood, and bone (Hindin et al., 2005; Wang et al., 2020). It was also reported that uranium polluted soils showed a negative ecological impact. Gongalsky (2003) reported that the diversity and macroinvertebrate abundance was reduced 3–37 times in the southeastern area of Siberia due to uranium pollution.

Uranium must be removed from a variety of aquatic environments, such as seawater, mine water, and other types of industrial wastewater utilized in effluent treatment for the nuclear industry. Various procedures such as chemical precipitation, ion exchange, membrane separation, adsorption is regularly used to clean up uranium-polluted wastewater (Gok and Aytas, 2009; Yue et al., 2021). Nevertheless, these approaches demonstrated lower efficacy and required higher costs in addition to the dangerous by-products resulting from the chemical methods (Yue et al., 2021). As an alternative to physical and chemical procedures, bioremediation procedure using biological materials such as bacteria or algal biomass are used which can be reliable, flexible, cheap, and user-friendly (Gavrilescu et al., 2009; Smječanin et al., 2022). More specifically, biosorption has grown in importance over the past two decades, showing remarkable potential as a low-cost, high-impact approach to environmental cleanup. The utilization of bacterial biomass as a biosorbent material for uranium removal or detoxification has been identified as a significant approach. This is mostly attributed to the advantageous characteristics of bacterial biomass, including its widespread availability, potential for reuse, and decreased operational expenses (Mahbub et al., 2016; Ikegami et al., 2020). Previous studies have reported that bacteria such as *Spirulina platensis*, *Nostoc linckia* (Cecal et al., 2012), *Anabaena flos-aquae* (Yuan et al., 2020), *Chlorella vulgaris* (Amini et al., 2013), *Chlamydomonas reinhardtii* (Erkaya et al., 2014), and *Bacillus subtilis* (Fowle et al., 2000), were used for uranium biosorption process. Several factors like pH, biomass dose, temperature, and concentration of metal ions have a great effect on biosorption rate (El-Naas et al., 2007; Bayramoglu et al., 2018; Ahmad et al., 2018). Therefore, there is a need for more investigations for the optimization conditions to efficiently uptake uranium from waste streams (El-Naas et al., 2007; Gok and Aytas, 2009).

The main goals of this research are to (1) assess *Bacillus* sp. strain MRS-1′s uranyl tolerance capacity, (2) examine the impact of pH, the temperature, biomass dose, initial uranyl quantity, and duration of contact on uranyl biosorption, and (3) assess the fit of the biosorption isotherm and kinetic mathematical models to experimental data. The *Bacillus* sp. strain MRS-1 bacterial strain employed in this research (ATCC 55673) was first obtained from a treatment plant for wastewater (Ibeanusi et al., 2003).

## 2. Materials and methods

### 2.1. Chemicals and reagents

The Luria broth (LB) utilized for the cultivation of bacteria was bought from Thomas Scientific, located in Swedesboro, NJ, USA. The Uranyl nitrate hexahydrate ACS, Reagent Grade was purchased from Electron Microscopy Sciences (Hatfield, PA, USA) and a stock solution of 100 g/L uranyl was set by dissolving Uranyl nitrate in sterile ultrapure Milli-Q water (Millipore Milli-Q System).

### 2.2. Minimum inhibitory concentration of uranyl against bacteria

The MIC of uranyl was determined by culturing *Bacillus* sp. strain MRS-1 bacteria (50 μL of an overnight culture) in sterile LB medium (5 mL) supplemented with varying final concentrations of uranyl ranging from 0 to 400 parts per million (ppm). This experiment was performed in triplicate using separate tubes. An incubator from New Brunswick Scientific was used to incubate the tubes at 25 °C for 24 h. The agitation speed in the incubator was maintained at a steady 150 revolutions per minute. After 24 h in culture, the Spectronic Genesys 2 Spectrophotometer was used to detect the absorbance of the sample at 600 nm. Uranyl's MIC, or minimum concentration, is characterized as the lowest concentration of the chemical on which the growth of the *Bacillus* sp. strain MRS-1 was inhibited.

### 2.3. Biomass preparation from bacteria for uranyl biosorption studies

Bacterial biomass was produced by inoculating 100 mL of LB medium with 1 mL of an overnight MRS-1 culture. After that, we allowed to grow overnight at 25 °C with a steady agitation speed of 150 revolutions per minute. The culture was transferred into a 50 mL falcon tube and subjected to centrifugation at the maximum speed (7142 g) using an Eppendorf 5430 R centrifuge for a duration of 10 min at a temperature of 4 °C in order to get viable biomass. The bacterial pellet underwent a washing process using sterile saline solution (0.9 % NaCl) and was subsequently suspended in the same saline solution at a concentration of 100 mg/mL.

### 2.4. Biosorption experiments

The biosorption tests were initially conducted using the LB medium. The findings of the study revealed that a substantial portion of the uranyl ions underwent precipitation inside the medium itself, independent of the presence of bacterial biomass. This observation suggests that some components of the LB medium interacted with the uranyl ions, resulting in their precipitation. Our previous research also indicated the formation of uranyl precipitation with the presence of nutrients such as phosphorous (Li et al., 2019). As a result, Milli-Q water was used in the subsequent trials as the medium for the biosorption tests.

Batch experiments were conducted to regulate the effect of different variables on the biosorption of uranyl. These factors included pH, temperature, beginning uranyl concentration, biomass dose, and contact period. The biosorption tests were performed using 10 mL of Milli-Q water that contained 10 ppm of uranyl, either with or without 1 g/L of *Bacillus* sp. strain MRS-1 bacterial biomass. The biosorption tests were performed in Falcon tubes with a capacity of 50 mL by incubating them in an incubator manufactured by New Brunswick Scientific. Experiments were conducted at 25 °C for 3 h with Milli-Q solutions of varied pH values (2, 4, 6, 7, 8, and 10) to assess the impact of pH on uranyl biosorption using *Bacillus* sp. strain MRS-1 bacteria. The effects of temperatures between 20 and 40 °C were investigated at a pH 7. The results of previous studies served as the foundation for this action. The impact of initial uranyl concentration on biosorption was then studied by applying concentrations of uranyl ranging from 1 to 50 ppm at a constant temperature of 20 °C.

We used biomass containing *Bacillus* sp. strain MRS-1 bacteria ranging from 0.5 g/L to 3.5 g/L to examine the influence of biomass dosage. In addition, the influence that various contact periods, ranging from 5 to 60 min, on the uranyl biosorption was investigated. For the purpose of ensuring the accuracy of the findings, every biosorption experiment was conducted using three sets of tubes simultaneously and was repeated twice.

### 2.5. Measurement of uranyl metal

The tubes containing the biosorption experiment were withdrawn from an Eppendorf 5430 R centrifuge after being centrifuged at the highest rate (7142 g) for five min at the ambient temperature (23 °C). The supernatant (5 mL) was transferred into 15 mL falcon tube, and 5 μL of yttrium has been included as a standard for internal use. The amount of uranyl metal in the supernatant was uncovered by assessing the intensity of the light produced by ionized plasma using an Optima 7000 inductively coupled plasma-optical emission spectrometry (ICP-OES) (Perkin Elmer, Waltham, MA, USA). Uranyl concentration in the solution was assessed using ICP with reference standards made from the exact identical stock solution used in the process of biosorption experiments.

### 2.6. Estimation of uranyl biosorption

To determine the uranyl biosorption rate (Q, %) and uranyl biosorption capacity (qe, mg/g), we utilized the following equations, as described in our previous study (Hoyle-Gardner et al., 2021). In our analysis, we subtracted the (C0 - Ce) value obtained from the tube without bacterium biomass from the (C0 - Ce) value obtained from the tube containing bacterium biomass. This subtraction allowed us to quantify the actual uranyl biosorption by the bacteria. These adjusted values were then applied in the equations below to calculate Q and qe:

$$Q = (C0 - Ce) / C0 * 100$$

$$qe = V * (C0 - Ce) / M$$

Here, the variables represent the following:

C0: Initial concentration of uranyl (mg/L).
Ce: Final concentration of uranyl.
V: Volume (L) of the solution.
M: Weight (g) of the bacterium biomass.

### 2.7. Isotherm and kinetic models

The batch experiment with varying starting uranyl concentrations was used to generate a plot of Ce/qe against Ce, which represents the Langmuir isotherm model for uranyl biosorption.

Below, we presented the Langmuir isotherm model in its linear version.

$$qe = qmaxbCe + bCe$$

Maximum uranyl uptake by the bacterial biomass is denoted by the trend of the Ce/qe versus Ce line graph, where Ce is the final concentration of uranyl in the mixture at the point of maximum adsorption and qe is the amount of uranyl uptake. It was demonstrated that the Freundlich isotherm model may be applied to the data on uranyl biosorption by plotting the data as a function of the equilibrium concentration vs the equilibrium capacity (Log qe versus Log Ce).

The Freundlich isotherm model in its linear version is seen below.

$$Log\ qe = Log\ Kf + 1/n\ Log\ Ce$$

At the time of maximum adsorption, the solution's final uranyl content, Ce, is equal to the bacterial biomass's maximum adsorption capacity, qe, in mg/g. Here, 'n' represents the Freundlich constant and 'Kf' represents the amount of adsorption or distribution coefficient. Values for 'n' and Kf may be estimated through examining the graph's slope and intercept.

Pseudo-first-order kinetics for bacteria biosorption of uranyl were elucidated by plotting the natural logarithm of (qe - qt) vs time (t) at different times. This equation was used to establish the pseudo-first-order model.

$$\log (qe - qt) = \log (qe - k1*t) / 2.303$$

In this context, qe represents the equilibrium adsorption capacity (mg of uranyl/g of adsorbent), qt is the adsorption capacity at a specific time t, and t denotes the elapsed time. The adsorption rate constant, k1, is expressed in units of liters per minute. From the experimental data, we derived the values for k1 (the pseudo-first-order adsorption rate constant, L/min) and qe.

To visualize the pseudo-second-order kinetic model for bacterial biosorption of uranyl, we plotted t/qt against time (t).

The following equation was used to get the pseudo second order model.

$$\text{The formula is: } t/qt = 1/k2 * qe2 + (1/qe) * t$$

### 2.8. FTIR spectroscopy and data analysis

The FTIR spectroscopy analysis was performed according to the previous report (Kepenek et al., 2019). After the biosorption assay, cell suspensions were centrifuged and cell pellets were resuspended in 15 μL of distilled water. FTIR spectroscopy measurements of bacterial samples were performed by JASCO 6800 FT-IR Spectrometer accompanied by a universal ATR unit that has one internal reflection since it contains diamond crystal. Air spectrum was used as background and subtracted to remove the atmospheric carbon dioxide and water absorption bands. Spectroscopic measurement of 5 μL sample was conducted at a resolution of 4 cm $-1$ at room temperature. Before taking spectroscopic measurements, sample was placed on a diamond/ZnSe crystal and was dried with a very mild $N_2$ flux for 5 min. Then the sample was scanned between the ranges of 6000–250 cm $-1$. For each sample, three replicates (5 μL each) were obtained from the original sample suspension (15 μL). Each replicate was independently scanned 100 times and averaged. The average spectra were used for further data analysis.

### 2.9. Statistical analysis for data processing

Using 'GraphPad Prism 3′, graphs were created and the mean standard deviation of three duplicate readings was used to present the biosorption test results. The kinetics models (pseudo-first second-order) along with the Langmuir and Freundlich models, were plotted for uranyl biosorption using Microsoft Excel (version 7). The least-squares method was applied to calculate the coefficient of determination, denoted as $R^2$. This value served as an indicator of how well the data confirmed to the respective models (Cruz et al., 2004).

## 3. Results

### 3.1. Bacillus sp. Strain MRS-1 bacterium uranyl tolerance study

The uranyl tolerance of *Bacillus* sp. strain MRS-1 was tested in this experiment by culturing the bacterium for 24 h at various uranyl concentrations. This bacterium showed a MIC of 400 ppm (1.68 mM) uranyl and can withstand up to 350 ppm uranyl, according to bacterial growth after 24 h (Fig. S1).

### 3.2. Biosorption studies

This batch experiment was designed to test the effect of pH on uranyl biosorption by the *Bacillus* sp. strain MRS-1 bacterium. Notably, it was noted that in the absence of bacterium, uranyl underwent precipitation inside the tubes at a pH level of 10. The present investigation revealed that the *Bacillus* sp. strain MRS-1 bacterium exhibited the highest level of uranyl biosorption at a pH value of 7 (Fig. 1).

The judgments of this study show that, in comparison to the other temperatures tested, *Bacillus* sp. strain MRS-1 had a higher uranyl

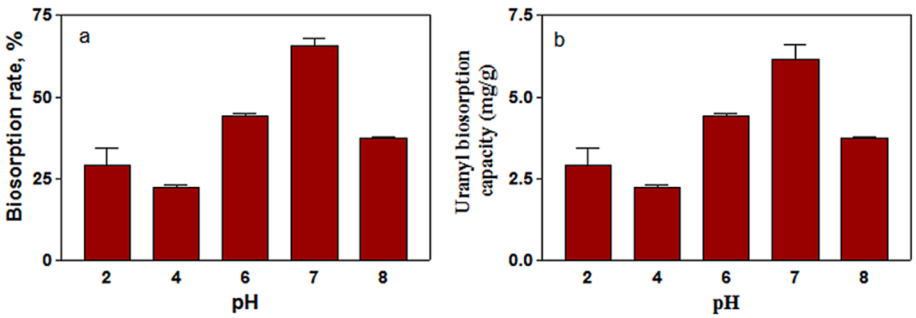


**Fig. 1.** Uranyl biosorption rate (a) and uranyl biosorption capacity (b) by MRS-1 *Bacillus* strain at various pH conditions.

biosorption rate and capacity at 20 °C (Fig. 2). The bacterium uranyl biosorption process has been observed to occur across a wide range of temperatures. The study of these data shows that the ideal temperature for the uranyl biosorption process varies with the kind of bacteria being employed.

The results of this research exhibit that, for uranyl starting concentrations between 1 and 25 ppm, the biosorption rate was mostly constant (Fig. 3a). On the other hand, when the initial uranyl content was increased from 1 to 50 ppm, the biosorption capacity showed a gradual rise (Fig. 3b). Because there were more metal ions within the available free active sites, the biosorption capacity enhanced gradually until all of the sites were filled by uranyl ions, at which point an equilibrium was attained. As Fig. 3a illustrates, the rate of biosorption significantly decreased when the initial uranyl concentration was 50 ppm.

When the bacterial biomass content was raised to 2 g/L, the biosorption rate increased significantly (Fig. 4a). The results showed that a biomass content of 2 g/L for the *Bacillus* sp. strain MRS-1 bacterium was optimal for uranyl biosorption. But as Fig. 4a shows, the biosorption rate drops as biomass concentration rises. Using a wet *Bacillus* sp. strain MRS-1 biomass dosage of 0.5 g/L, the greatest uranyl adsorption capacity of 5.5 ± 0.46 mg/g was reported in the experiments (Fig. 4b).

One important aspect affecting the rate of biosorption is the length of time that uranyl ions in the solution interact with the bacteria; this rate is dependent on the uranyl affinity of the bacteria. The biosorption process began within 5 min, according to the current experiment, and increased over the next 30 min, peaking at that point (Fig. 5). After then, the entire process attained a condition of balance and continued to run continuously for another half hour. The observed progression from 0 to 30 min may be attributed to uranyl binding to the empty active sites on the surface of bacterial cells. It is plausible that uranyl ions occupied these active areas within half an hour. Consequently, the biosorption rate and capacity reached a plateau as there were no vacant active sites left for uranyl binding on the bacterial cell surface. The relatively shorter contact time observed in this study could be attributed to the higher bacterial biomass concentration of 1 g/L used in the biosorption experiment.

### 3.3. Isotherm and kinetic model analysis

Isotherm models were used to analyze the experimental data and draw conclusions about the bacterial capacity for uranyl biosorption. As demonstrated in Fig. 6, this study illustrates the application of the Freundlich and Langmuir equilibrium models in estimating uranyl biosorption by *Bacillus* sp. strain MRS-1 bacteria.

The application of the Langmuir model resulted in a maximum biosorption capacity (qmax) of 24.5 mg/g, as shown in Table 1. This capacity range of uranyl adsorption by MRS-1 bacteria is consistent with that of other *Bacillus* species reported in previous studies (refer to Table 3). The analysis of equilibrium models indicated that the Freundlich coefficient (n) was greater than 1. The calculated $R^2$ values of 0.98 and 0.94 for the Freundlich and Langmuir equilibrium models, respectively, imply that these models aptly fit the uranyl biosorption process by *Bacillus* sp. strain MRS-1 bacterium (Table 1; Fig. 6).

The $R^2$ values among the pseudo-first-order and pseudo-second-order kinetic models in this investigation were 0.25 and 0.99, respectively, indicating that the pseudo-second-order kinetic model best describes the uranyl biosorption kinetics (Table 2; Fig. 6).

Chemical adsorption is assumed to be the rate-limiting step in the pseudo-second-order kinetic model. Various uranyl affinities were found on the outermost layer of *Bacillus* sp. strain MRS-1 bacteria as determined by the biosorption isotherms examined in this work (Fig. 6), highlighting the importance of *Bacillus* sp. strain MRS-1 bacteria's adsorption capacity in uranyl biosorption.

### 3.4. FTIR analysis

The shifts and stretches in the FTIR analysis from 250 to 6000 represent some of the functional groups which are involved in mercury

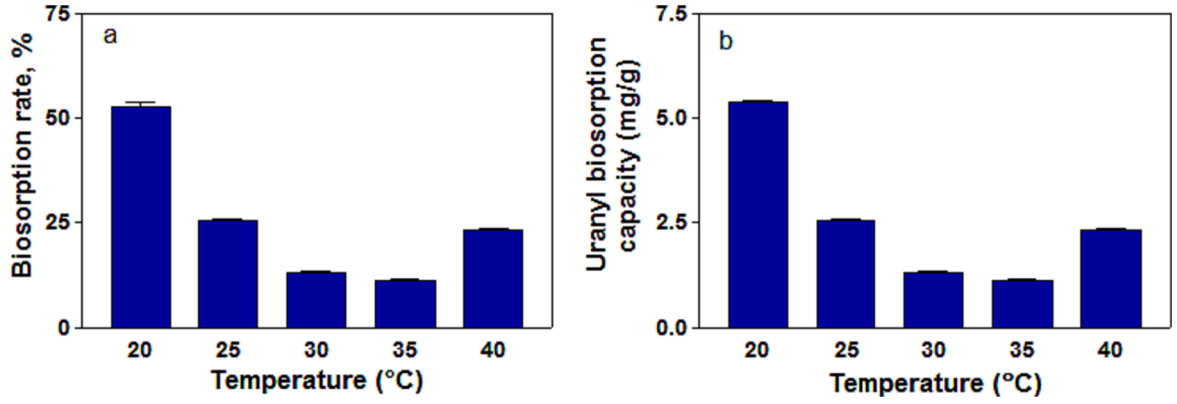


**Fig. 2.** Uranyl biosorption rate (a) and uranyl biosorption capacity (b) by MRS-1 *Bacillus* strain under various temperature conditions.

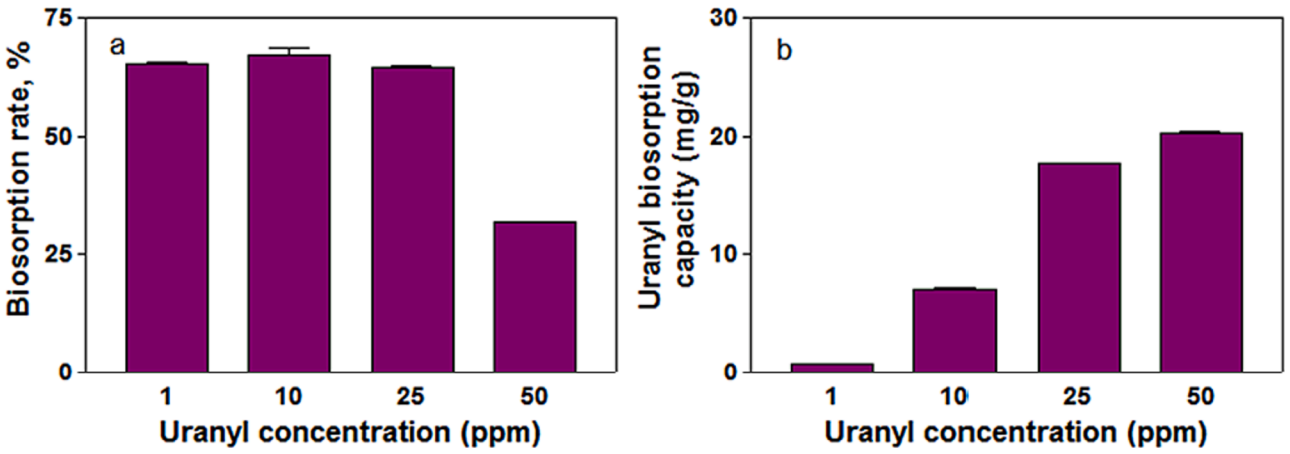


**Fig. 3.** Uranyl biosorption rate (a) and uranyl biosorption capacity (b) by MRS-1 *Bacillus* strain under various initial uranyl concentrations.

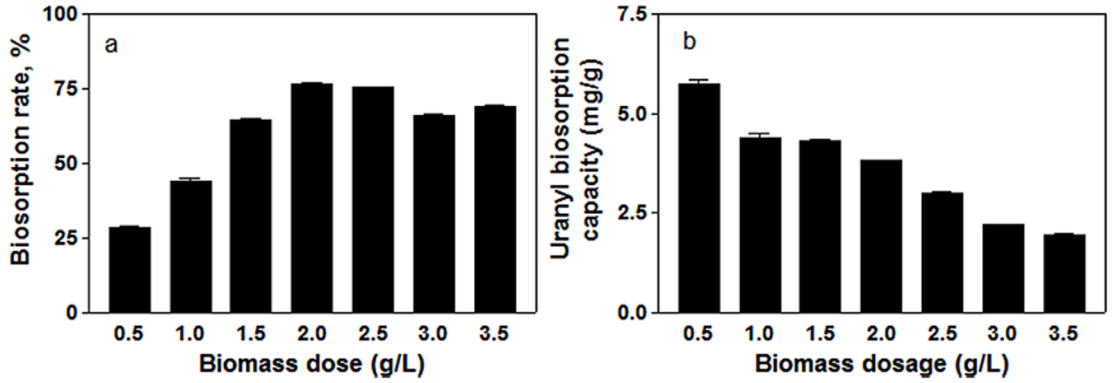


**Fig. 4.** Uranyl biosorption rate (a) and uranyl biosorption capacity (b) by MRS-1 *Bacillus* strain under various biomass dose conditions.

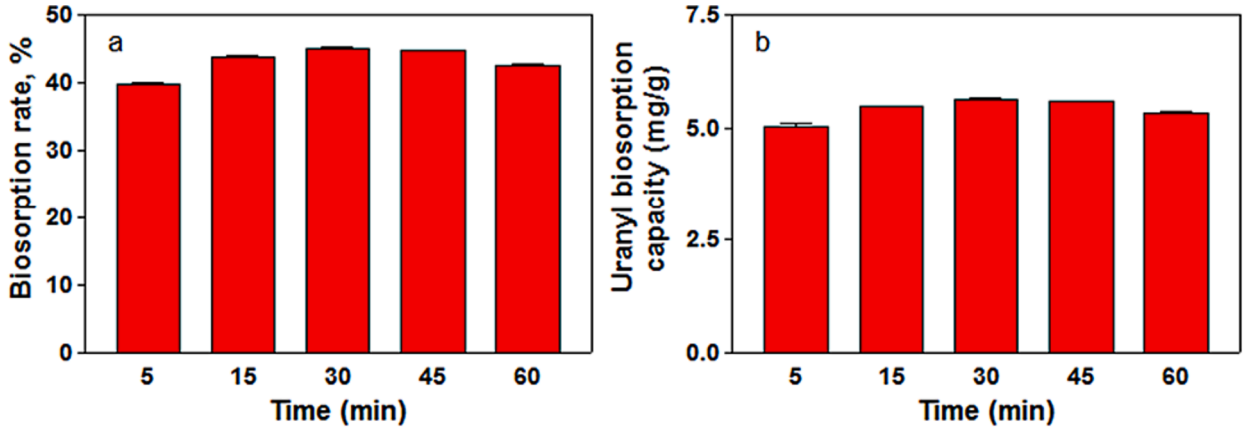


**Fig. 5.** Uranyl biosorption rate (a), uranyl biosorption capacity (b) by MRS-1 *Bacillus* strain under various time points.

uptake in the given bacterial strain (Fig. 7). These shifts/sharping of peaks (1081–3304 cm $^{-1}$) are prominent in stress condition compared to control one. These functional group could be hydroxyl, amino, carboxyl. The peaks sharping at 1081–2346 represent phosphate ($PO_2$), amide and carboxyl group. 3278 to 2851 cm$^{-1}$ changes are due to hydroxyl and amide stretching. 1741 to 1220 cm$^{-1}$ changes are due to proteins and peptide amide linkages attraction. 1228 to 1038 cm$^{-1}$ peaks shift and sharpening aliphatic amine having stretched of C-N and C-O stretching belongs to ester, ether carboxylic acid and alcohols. The –C = O has strong bond with peaks in range of 1742–1242 while –CH group interacts with peaks at 2928 in the spectra of FTIR. The alcohols and carboxylic acid have C-O group which stretched in the range of 1042–1059.

## 4. Discussion

Heavy metal contamination has recently been identified as one of the most pressing environmental issues on a worldwide scale. Uranium is a naturally occurring radionuclide and less abundant heavy metal. However, anthropogenic sources such as coal combustion and nuclear plants are responsible for the increased uranium. So it can be remediating by using uranium resistant bacteria. In this study the uranium resistant

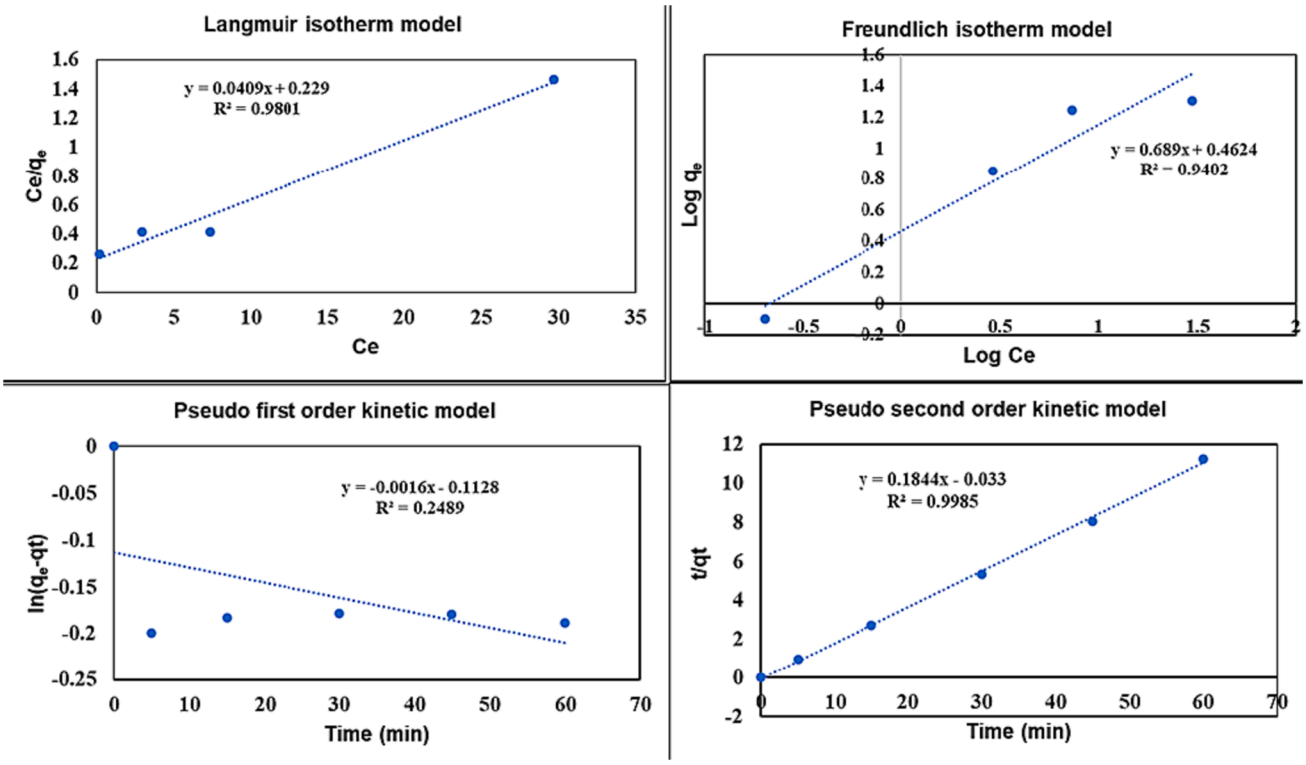


**Fig. 6.** Langmuir, Freundlich isotherm (top) and pseudo first order, pseudo second order kinetic (bottom) models for the biosorption of uranyl by MRS-1 *Bacillus* strain.

**Table 1**
Langmuir and Freundlich isotherm model parameters for uranyl biosorption by *Bacillus* MRS-1 bacterium.

| Langmuir | | | Freundlich | | |
|---|---|---|---|---|---|
| KL | $q_{max}$ (mg/g) | $R^2$ | Kf | n | $R^2$ |
| 106.7549 | 24.5 | 0.98 | 2.89 | 1.45 | 0.94 |

**Table 2**
Pseudo first order and second order kinetic model parameters for uranyl biosorption by *Bacillus* MRS-1 bacterium.

| Pseudo first order | | | Pseudo second order | | |
|---|---|---|---|---|---|
| K1 | qe (mg/g) | $R^2$ | K2 | qe (mg/g) | $R^2$ |
| $-2.7x10^{-5}$ | 0.893 | 0.249 | −1.031 | 5.42 | 0.99 |

**Table 3**
Uranium biosorption capacity with various *Bacillus* species.

| Biosorbent | Biosorption conditions | Maximum uranium biosorption capacitymg/g | Reference |
|---|---|---|---|
| *Bacillus cereus* MRS-1 strain | pH 7, 20 °C, 30 min | 24.5 | This study |
| *Bacillus subtilis* | pH 4.5, 25 °C | 90.91 | Yao et al., 2016 |
| *Bacillus mojavensis* | pH 4–7 | 25.8 | Özdemir et al., 2017b |
| *Bacillus vallismortis* | pH 4–5 | 23.6 | Özdemir et al., 2017a |
| *Bacillus* sp. dwc-2 | pH 3, 30 °C, 12 h | 6.3 | Li et al., 2014 |
| *Bacillus subtilis* | pH 6, 20 °C, 3 h | 376.64 | Tong 2017 |
| *Bacillus amyloliquefaciens* | pH 6, 30 °C | 179.5 | Liu et al., 2019 |

bacterium was used for its bioremediation. It was reported that *Bacillus vallismortis* showed MIC value of U(VI) 85 mg/L and 15 mg/L in liquid and solid medium, respectively (Özdemir et al., 2017a). It was also reported that another strain *Bacillus mojavensis* showed MIC of 5 mg/L U (VI) after 24 h (Özdemir et al., 2017b). In this study, *Bacillus* sp. strain MRS-1 showed higher MIC for uranyl than the other thermotolerant *Bacillus* strains used for uranium biosorption (Ozdemir et al., 2017a; Özdemir et al., 2017b).

The research aim was to identify the parameters that effect the adsorption of uranyl by a *Bacillus* sp. strain MRS-1 that is resistant to metals. Initial uranyl concentration, interaction duration, biomass dose, temperature, and pH were some of the variables examined. Since the biosorption process relies on the relations of metal ions with certain structural groups on bacteria's cell surfaces, the solution's pH is crucial (Tunali et al., 2006; El-Moselhy et al., 2013). There is a chance that ions of metals and the bacterial cell wall receptors will be strongly attracted to one another at a pH that is neither acidic nor basic (Ren et al., 2015). This finding showed concordance with other bacteria reported in prior studies (Carvajal et al., 2012, Özdemir et al., 2017a). Nonetheless, prior research utilizing a variety of bacterial species, such as *Streptomyces levaris* and *Pseudomonas aeruginosa* strain CSU, has shown a presence of uranyl biosorption in an acidic pH range (Hu et al., 1996, Li et al., 2014). Thus, the bacterial species determines whether uranyl can be biosynthesized at a certain pH, indicating differences in the receptors on bacterial surface that bind uranyl.

Critical to the biosorption process is the temperature at which incubation takes place during the interaction of bacteria with metal ions (Panda et al., 2006). Previous investigations making use of bacterial strains of *P. aeruginosa* and *Rhodotorula glutinis* have shown that the maximum degree of biosorption was seen at a temperature of 22 °C (Bai et al., 2012; Li et al., 2014). The starting concentration of uranyl, a catalyst for transfer of mass in biosorption studies, affects the biosorption process. For example, (Saleh et al., 2013; Ren et al., 2015). Uranyl concentration was significantly reduced at 50 ppm, which might

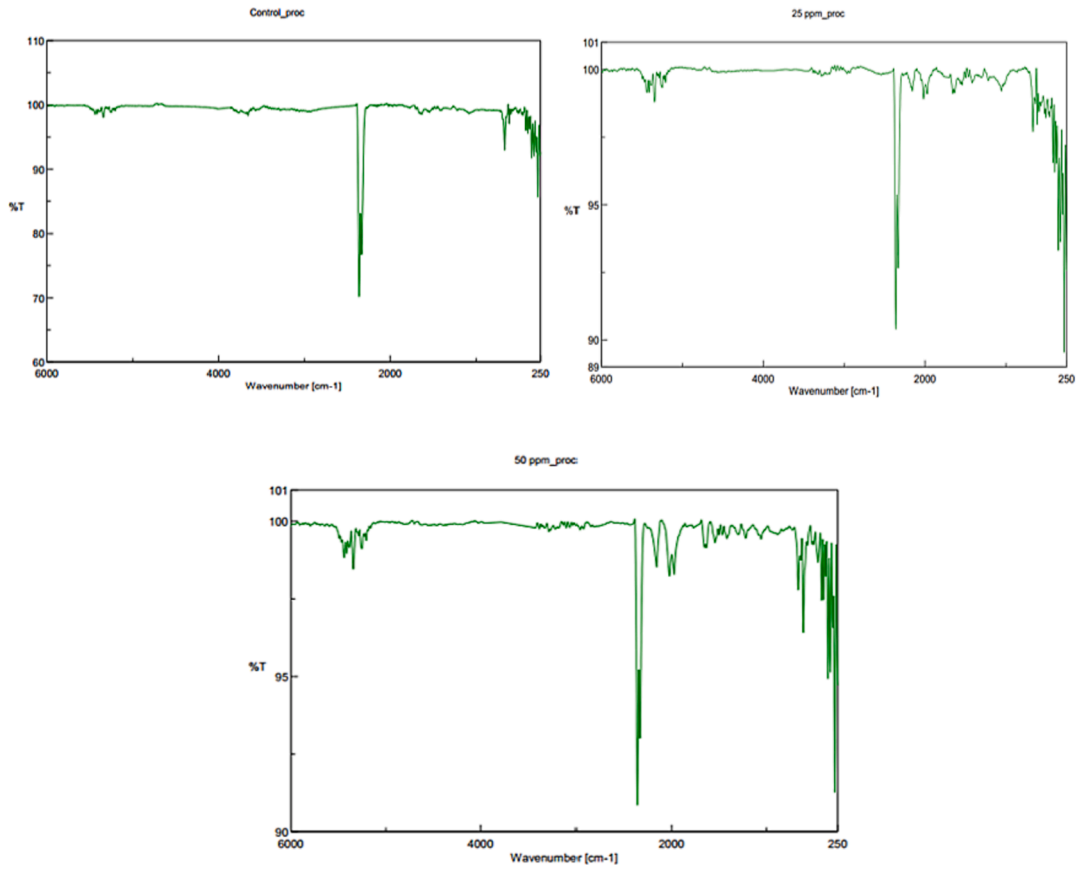


**Fig. 7.** FTIR Analysis of Mercury resistant bacteria with (25, 50 ppm) and without stress of mercury.

be explained by the lack or restricted availability of vacant active sites on the surface of bacterial cells after equilibrium is established (Wierzba and Latala, 2010). It is possible that the state of biosorption equilibrium was attained at a uranyl initial concentration below 50 ppm (Ho and Mckay, 2000). Multiple mechanisms, such as surface the adsorption ion exchange, collaboration, chelation, micro-precipitation, and the presence or absence of groups with functions in bacterial biomass, all have a role in determining the biosorption rate (Yeo et al., 2008; Mittal et al., 2009). Previous research has indicated that elevated biomass leads to a proportional increase in open receptors on the bacterial surface, facilitating uranyl ion binding (Mittal et al., 2009; Ren et al., 2015). The results showed that a biomass content of 2 g/L for the *Bacillus* sp. strain MRS-1 bacteria was optimal for uranyl biosorption. It may be deduced that the ability to adsorb metals depends on the particular bacteria that was used in the uranyl biosorption experiment. This conclusion coincides with the wide variety in uranyl adsorption capabilities shown by various bacteria, as reported in the review (Kolhe et al., 2018). The previous review article on uranyl biosorption showed that, depending on the bacterial species involved, the equilibrium period for uranyl adsorption by various bacteria differed at different time intervals (Kolhe et al., 2018).

Bacterial capacity for uranyl biosorption was determined by using isotherm model. Researchers have commonly utilized the Freundlich and Langmuir equilibrium models to evaluate various metal biosorption studies, including uranyl biosorption (Ren et al., 2015; Hoyle-Gardner et al., 2021). The analysis of equilibrium models indicated that the Freundlich coefficient (n) was greater than 1, suggesting advantageous uranyl biosorption under the studied conditions, consistent with prior literature findings (Mohapatra et al., 2019). These findings are consistent with those reported in the literature (Kolhe et al., 2018) in which several bacteria demonstrated uranyl biosorption behavior that could be characterized by the pseudo-second-order kinetic model, the Freundlich equilibrium model, and the Langmuir equilibrium model. The $R^2$ values among the pseudo-first-order and pseudo-second-order kinetic models in this investigation were 0.25 and 0.99, respectively. In contrast to the Langmuir model, which assumes uniform forces similar to chemical reaction forces during monolayer biosorption, the Freundlich isotherm model predicts a surface with varied affinities, which in turn leads to metal ion the biosorption (Bulgariu et al., 2013). The shifts/sharping of peaks (1081–3304 $cm^{-1}$) are prominent in stress condition compared to control one. These functional group could be hydroxyl, amino, carboxyl. So, the FTIR finding of this study was similar to previous studies.

### *4.1. Limitations of the study*

The current *Bacillus* sp. strain MRS-1 was analyzed for its biosorption rate/capacity only in laboratory scale experiments, not in natural environment conditions. In our current studies, we didn't study the biosorption of uranyl in the presence of other heavy metals, e.g., arsenic, chromium, cadmium. It was reported earlier that the presence of other metal ions in the solution, besides the metal of interest, may interfere the biosorption process (Amini et al., 2013).

## 5. Conclusions

The *Bacillus* sp. strain MRS-1 bacterium exhibited MIC of 400 ppm for uranyl. The highest uranyl biosorption rate and the capacity was found in studies using a pH 7, 20 °C temperature, and a 30 min contact duration. This bacterium strain has ideal biosorption rate and biosorption capacity for uranyl which was further best described by the pseudo-second order kinetic model, and both Freundlich and Langmuir isotherms. The FTIR analysis showed the interaction of different functional groups on bacterial cell surface with the uranyl in the surrounding. All the experiments related to biosorption rate, capacity and FTIR

analysis make it clear that the isolated bacterium is an ideal candidate for uranyl biosorption. So, this bacterium strain can be used as a potential agent for uranyl bioremediation from contaminated sites due to its high uranyl biosorption rate.

## Funding information

This work was supported by the Department of Energy Minority Serving Institution Partnership Program (MSIPP) managed by the Savannah River National Laboratory under SRNS contract SOW#G-SOW-A-02188; TOA/PO: NO 0000456319 and Florida A&M University Title III program.

## Declaration of competing interest

The authors declare that they have no known competing financial interests or personal relationships that could have appeared to influence the work reported in this paper.

## Acknowledgements

The authors would like to acknowledge Dr. Ramesh B Badisa (College of Pharmacy and Pharmaceutical Sciences, Florida A&M University) for formatting the figures and Dr. J.S. Raaj Vellore Winfred (Materials Characterization Laboratory, Department of Chemistry & Biochemistry, Florida State university) for the FTIR analysis.

## Appendix A. Supplementary data

Supplementary data to this article can be found online at https://doi.org/10.1016/j.sjbs.2023.103873.

## References

Ahmad, A., Bhat, A.H., Buang, A., 2018. Biosorption of transition metals by freely suspended and Ca-alginate immobilised with Chlorella vulgaris: kinetic and equilibrium modeling. J Clean Prod 171, 1361–1375.

Ali, W., Aslam, M.W., Feng, C., Junaid, M., Ali, K., Li, S., et al., 2019. Unraveling prevalence and public health risks of arsenic, uranium and co-occurring trace metals in groundwater along riverine ecosystem in Sindh and Punjab, Pakistan. Environ Geochem Health 41, 2223–2238.

Amini, M., Younesi, H., Bahramifar, N., 2013. Biosorption of U (VI) from aqueous solution by Chlorella vulgaris: equilibrium, kinetic, and thermodynamic studies. J Environ Eng 139 (3), 410–421.

Bai, J., Wu, X., Fan, F., Tian, W., Yin, X., Zhao, L., et al., 2012. Biosorption of uranium by magnetically modified Rhodotorula glutinis. Enzyme Microb. Technol. 51 (6–7), 382–387.

Bayramoglu, G., Akbulut, A., Acıkgoz-Erkaya, I., Yakup, A.M., 2018. Uranium sorption by native and nitrilotriacetate-modifed Bangia atropurpurea biomass: kinetics and thermodynamics. J Appl Phycol 30, 649–661.

Bjørklund, G., Semenova, Y., Pivina, L., Dadar, M., Rahman, M., Aaseth, J., Chirumbolo, S., 2020. Uranium in drinking water: a public health threat. Arch. Toxicol 94 (5), 1551–1560.

Bulgariu, L., Lupea, M., Bulgariu, D., Rusu, C., Macoveanu, M., 2013. Equilibrium study of Pb (II) and Cd (II) biosorption from aqueous solution on marine green algae biomass. Environmental Engineering & Management Journal (EEMJ) 12 (1).

Carvajal, D.A., Katsenovich, Y.P., Lagos, L.E., 2012. The effects of aqueous bicarbonate and calcium ions on uranium biosorption by Arthrobacter G975 strain. Chem. Geol. 330, 51–59.

Cecal, A., Humelnicu, D., Rudic, V., Cepoi, L., Ganju, D., Cojocari, A., 2012. Uptake of uranyl ions from uranium ores and sludges by means of Spirulina platensis, Porphyridium cruentum and Nostok linckia alga. Bioresour Technol 118, 19–23.

Choppin, G., Liljenzin, J., Rydberg, J., Ekberg, C., 2013. Mechanisms and Models of Nuclear. Reactions. https://doi.org/10.1016/B978-0-12-405897-2.00011-2.

Coyte, R.M., Vengosh, A., 2020. Factors controlling the risks of co-occurrence of the redox-sensitive elements of arsenic, chromium, vanadium, and uranium in groundwater from the Eastern United States. Environ Sci Technol 54 (7), 4367–4375.

Cruz, C.C., Da Costa, A.C.A., Henriques, C.A., Luna, A.S., 2004. Kinetic modeling and equilibrium studies during cadmium biosorption by dead Sargassum sp. biomass. Bioresour. Technol. 91 (3), 249–257.

Cumberland, S.A., Douglas, G., Grice, K., Moreau, J.W., 2016. Uranium mobility in organic matter-rich sediments: A review of geological and geochemical processes. Earth Sci. Rev. 159, 160–185.

Echevarria, G., Sheppard, M.I., Morel, J., 2001. Effect of pH on the sorption of uranium in soils. J. Environ. Radioact. 53 (2), 257–264.

EFSA, 2009. Scientifc opinion of the panel on contaminants in the food chain on a request from German federal institute for risk assessment (BfR) on uranium in foodstufs, in particular mineral water. EFSA J, 1018, 1–59.

El-Moselhy, K.M., Shaaban, M.T., Ibrahim, H.A., Abdel-Mongy, A.S., 2013. Biosorption of cadmium by the multiple-metal resistant marine bacterium Alteromonas macleodii ASC1 isolated from Hurghada harbour, Red Sea. Arch Sci 66 (2), 259–272.

El-Naas, M.H., Al-Rub, F.A., Ashou, I., Al Marzouqi, M., 2007. Efect of competitive interference on the biosorption of lead (II) by Chlorella vulgaris. Chem Eng Process: Process Intensifcation 46 (12), 1391–1399.

Erkaya, I.A., Arica, M.Y., Akbulut, A., Bayramoglu, G., 2014. Biosorption of uranium (VI) by free and entrapped Chlamydomonas reinhardtii: kinetic, equilibrium and thermodynamic studies. J Radioanal Nucl Chem 299 (3), 1993–2003.

Filistovic, V., Maceika, E., Tarasiuk, N., Luksiene, B., Konstantinova, M., Buivydas, S., Koviazina, E., Puzas, A., 2015. Model of non-equilibrium multiphase contaminant transport in lake water-sediment system. Water Air Soil Pollut 226 (6), 202.

Fowle, D.A., Fein, J.B., Martin, A.M., 2000. Experimental study of uranyl adsorption onto *Bacillus subtilis*. Environ Sci Technol 34, 3737–3741.

Gao, N., Huang, Z., Liu, H., Hou, J., Liu, X., 2019. Advances on the toxicity of uranium to different organisms. Chemosphere 237, 124548.

Gavrilescu, M., Pavel, L.V., Cretescu, I., 2009. Characterization and remediation of soils contaminated with uranium. J Hazard Mater 163 (2–3), 475–510.

Godoy, J.M., Ferreira, P.R., de Souza, E.M., da Silva, L., Bittencourt, I.C.S., Fraifeld, F., 2019. High uranium concentrations in the groundwater of the Rio de Janeiro State, Brazil, mountainous region. J Braz Chem Soc 30, 224–233.

Gok, C., Aytas, S., 2009. Biosorption of uranium (VI) from aqueous solution using calcium alginate beads. J Hazard Mater 168 (1), 369–375.

Gongalsky, K.B., 2003. Impact of pollution caused by uranium production on soil macrofauna. Environ Monit Assess 89 (2), 197–219.

Hindin, R., Brugge, D., Panikkar, B., 2005. Teratogenicity of depleted uranium aerosols: a review from an epidemiological perspective. Environ. Health 4, 1–19.

Ho, Y.S., McKay, G., 2000. The kinetics of sorption of divalent metal ions onto sphagnum moss peat. Water Res. 34 (3), 735–742.

Hoyle-Gardner, J., Jones, W., Badisa, V.L., Mwashote, B., Ibeanusi, V., Gaines, T., Tucker, L., 2021. Lead metal biosorption and isotherms studies by metal-resistant Bacillus strain MRS-2 bacterium. J. Basic Microbiol. 61 (8), 697–708.

Hu, M.Z.C., Norman, J.M., Faison, B.D., Reeves, M.E., 1996. Biosorption of uranium by Pseudomonas aeruginosa strain CSU: characterization and comparison studies. Biotechnol. Bioeng. 51 (2), 237–247.

Ibeanusi, V.M., Phinney, D., Thompson, M., 2003. Removal and recovery of metals from a coal pile runoff. Environ. Monit. Assess. 84, 35–44.

Ikegami, K., Hirose, Y., Sakashita, H., Maruyama, R., Sugiyama, T., 2020. Role of polyphenol in sugarcane molasses as a nutrient for hexavalent chromium bioremediation using bacteria. Chemosphere 250, 126267.

Ivanova, K., Stojanovska, Z., Badulin, V., Kunovska, B., Yovcheva, M., 2015. Radiological impact of surface water and sediment near uranium mining sites. J Radiol Prot 35 (4), 819–834.

Kepenek, E.S., Gozen, A.G., Severcan, F., 2019. Molecular characterization of acutely and gradually heavy metal acclimated aquatic bacteria by FTIR spectraoscopy. J Biophotonics 12 (5), e201800301.

Kolhe, N., Zinjarde, S., Acharya, C., 2018. Responses exhibited by various microbial groups relevant to uranium exposure. Biotechnol. Adv. 36 (7), 1828–1846.

Lakaniemi, A.-M., Douglas, G.B., Kaksonen, A.H., 2019. Engineering and kinetic aspects of bacterial uranium reduction for the remediation of uranium contaminated environments. J. Hazard. Mater. 371, 198–212.

Li, X., Ding, C., Liao, J., Lan, T., Li, F., Zhang, D., Tang, J., 2014b. Biosorption of uranium on Bacillus sp. dwc-2: preliminary investigation on mechanism. J. Environ. Radioact. 135, 6–12.

Li, R., Ibeanusi, V., Hoyle-Gardner, J., Crandall, C., Jagoe, C., Seaman, J., et al., 2019. Bacterial-facilitated uranium transport in the presence of phytate at Savannah River Site. Chemosphere 223, 351–357.

Li, D., Seaman, J.C., Chang, H.-S., Jaffe, P.R., van Groos, P.K., Jiang, D.-T., Pan, Y., 2014a. Retention and chemical speciation of uranium in an oxidized wetland sediment from the Savannah River Site. J. Environ. Radioact. 131, 40–46.

Liesch, T., Hinrichsen, S., Goldscheider, N., 2015. Uranium in groundwater-fertilizers versus geogenic sources. Sci Total Environ 536, 981–995.

Mahbub, K.R., Krishnan, K., Megharaj, M., Naidu, R., 2016. Bioremediation potential of a highly mercury resistant bacterial strain Sphingobium SA2 isolated from contaminated soil. Chemosphere 144, 330–337.

Malikova, I.N., Strakhovenko, V.D., Ustinov, M.T., 2020. Uranium and thorium contents in soils and bottom sediments of lake Bolshoye Yarovoye, western Siberia. J Environ Radioact 211, 106048.

Matteoda, E.M., Blarasin, M.T., Lutri, V., Giacobone, D., 2019. Uranium in groundwater in the sedimentary aquifer of the eastern sector of valle de La cruz, Cordoba, Argentina. Intern J Eng Appl Sci 6, 20–25.

Mittal, A., Kaur, D., Malviya, A., Mittal, J., Gupta, V., 2009. Adsorption studies on the removal of coloring agent phenol red from wastewater using waste materials as adsorbents. J. Colloid Interface Sci. 337 (2), 345–354.

Mohapatra, R.K., Parhi, P.K., Pandey, S., Bindhani, B.K., Thatoi, H., Panda, C.R., 2019. Active and passive biosorption of Pb (II) using live and dead biomass of marine bacterium Bacillus xiamenensis PbRPSD202: Kinetics and isotherm studies. J. Environ. Manage. 247, 121–134.

Ozdemir, S., Oduncu, M.K., Kilinc, E., Soylak, M., 2017a. Resistance, bioaccumulation and solid phase extraction of uranium (VI) by Bacillus vallismortis and its UV–vis spectrophotometric determination. J. Environ. Radioact. 171, 217–225.

Özdemir, S., Oduncu, M.K., Kilinc, E., Soylak, M., 2017b. Tolerance and bioaccumulation of U (VI) by Bacillus mojavensis and its solid phase preconcentration by Bacillus

mojavensis immobilized multiwalled carbon nanotube. J. Environ. Manage. 187, 490–496.
Panda, G., Das, S., Chatterjee, S., Maity, P., Bandopadhyay, T., Guha, A., 2006. Adsorption of cadmium on husk of *Lathyrus sativus*: Physico-chemical study. Colloids Surf. B Biointerfaces 50 (1), 49–54.
Pant, D., Keesari, T., Roy, A., Sinha, U.K., Singh, M., Jain, S.K., Tripathi, R.M., 2019. Study on groundwater quality in parts of Rajasthan with special reference to uranium contamination. J Radioanal Nucl Chem 322, 165–171.
Portela, J.F., de Souza, J.P.R., Tonha, M.D., Bernardi, J.V.E., Garnier, J., SouzaDe, J.R., 2020. Evaluation of total mercury in sediments of the Descoberto River Environmental Protection Area-Brazil. Int J Environ Res Public Health 17 (1), 154.
Ren, G., Jin, Y., Zhang, C., Gu, H., Qu, J., 2015. Characteristics of *Bacillus* sp. PZ-1 and its biosorption to Pb (II). Ecotoxicol. Environ. Saf. 117, 141–148.
Roper, A.R., Stabin, M.G., Delapp, R.C., Kosson, D.S., 2013. Analysis of naturally-occurring radionuclides in coal combustion fly ash, gypsum, and scrubber residue samples. Health Phys. 104 (3), 264–269.
Rump, A., Eder, S., Lamkowski, A., Hermann, C., Abend, M., Port, M., 2019. A quantitative comparison of the chemo-and radiotoxicity of uranium at different enrichment grades. Toxicol. Lett. 313, 159–168.
Saleh, T.A., Gupta, V.K., Al-Saadi, A.A., 2013. Adsorption of lead ions from aqueous solution using porous carbon derived from rubber tires: experimental and computational study. J. Colloid Interface Sci. 396, 264–269.
Sayadi, M.H., Sayyed, M.R.G., Kumar, S., 2010. Short-term accumulative signatures of heavy metals in river bed sediments in the industrial area, Tehran, Iran. Environ Monit Assess 162 (1–4), 465–473.
Schnug, E., & Lottermoser, B.G. 2013. Fertilizer-derived uranium and its threat to human health. Environ Sci Technol, 19;47(6), 2433-2434.
Smječanin, N., Bužo, D., Mašić, E., Nuhanović, M., Sulejmanović, J., Azhar, O., Sher, F., 2022. Algae based green biocomposites for uranium removal from wastewater: kinetic, equilibrium and thermodynamic studies. Mater Chem Phys 283, 125998.
Tunali, S., Çabuk, A., Akar, T., 2006. Removal of lead and copper ions from aqueous solutions by bacterial strain isolated from soil. Chem. Eng. J. 115 (3), 203–211.
Wang, S., Ran, Y., Lu, B., Li, J., Kuang, H., Gong, L., Hao, Y., 2020. A review of uranium-induced reproductive toxicity. Biol. Trace Elem. Res. 196, 204–213.
Wierzba, S., Latała, A., 2010. Biosorption lead (II) and nikel (II) from an aqueous solution by bacterial biomass. Pol. J. Chem. Technol. 12 (3), 72–78.
Yeo, I.W., Roh, Y., Lee, K., Jung, C.M., 2008. Arsenic reduction and precipitation by *Shewanella* sp.: batch and column tests. Geosci J 12, 151–157.
Yuan, Y., Liu, N., Dai, Y., Wang, B., Liu, Y., Chen, C., Huang, D., 2020. Effective biosorption of uranium from aqueous solution by cyanobacterium *Anabaena fos-aquae*. Environ Sci Pollut Res 27 (35), 44306–44313.
Yue, Z., Dexin, D., Guangyue, L., Haitao, Y., Kaige, Z., Nan, H., 2021. Enhanced efects and mechanisms of *Syngonium podophyllum-Peperomia tetraphylla* co-planting on phytoremediation of low concentration uraniumbearing wastewater. Chemosphere 279, 130810.
Zahra, A., Hashmi, M.Z., Malik, R.N., Ahmed, Z., 2014. Enrichment and geo-accumulation of heavy metals and risk assessment of sediments of the Kurang Nallah-Feeding tributary of the Rawal Lake Reservoir, Pakistan. Sci Total Environ 470, 925–933.